Mineralogy and Petrology (1993) 48: 235–255

Mineralogy and Petrology

Cesstibtantite—a Geologic Introduction to the Inverse Pyrochlores

T. S. Ercit[1], P. Černý[2], and F. C. Hawthorne[2]

[1] Research Division, Canadian Museum of Nature, Ottawa, Canada
[2] Department of Geological Sciences, University of Manitoba, Winnipeg, Canada

With 5 Figures

Received September 24, 1992;
accepted January 14, 1993

Summary

The crystal structure of cesstibtantite has been solved from diffractometer data collected on samples from Leshaia, Russia and the Tanco pegmatite, Manitoba. Cesstibtantite from the Leshaia pegmatite (type locality) has a 10.515(2) Å, space group $Fd3m$, composition $Cs_{0.31}(Sb_{0.57}Na_{0.31}Pb_{0.02}Bi_{0.01})_{\Sigma 0.91}(Ta_{1.88}Nb_{0.12})_{\Sigma 2}(O_{5.69}[OH, F]_{0.31})_{\Sigma 6}(OH, F)_{0.69}$, Z 8; its structure was refined to R 3.8, wR 4.3% using 96 observed ($F > 3\sigma[F]$) reflections (Mo$K\alpha$). Cesstibtantite from the Tanco pegmatite has a 10.496(1) Å, space group $Fd3m$, composition $(Cs_{0.22}K_{0.01})_{\Sigma 0.23}(Na_{0.45}Sb_{0.39}Pb_{0.14} \cdot Ca_{0.06}Bi_{0.02})_{\Sigma 1.06}(Ta_{1.95}Nb_{0.05})_{\Sigma 2}(O_{5.78}[OH, F]_{0.22})_{\Sigma 6}(OH, F)_{0.55}$, Z 8; its structure was refined to R 3.9 wR 3.7% using 104 observed reflections. Cesstibtantite differs from the normal pyrochlores in that it contains significant amounts of very large cations such as Cs. As these cations are too large ($^{VIII}[r] > 1.60$ Å) for the conventional [8]-coordinated A site, they occupy the [18]-coordinated ϕ site, which normally contains monovalent anions. Natural cesstibtantite samples are non-ideal in that both Cs and monovalent anions occur at the ϕ site; thus cesstibtantite is intermediate to the *normal pyrochlores* (with only monovalent anions at the ϕ site) and the *inverse pyrochlores* (with only large cations at the ϕ site).

Zusammenfassung

Cesstibtantit—eine geologische Einführung in die inversen Pyrochlore

Die Kristallstruktur von Cesstibtantit wurde auf der Basis von Diffraktometerdaten von Proben von Leshaia, Russland und dem Tanco Pegmatit, Manitoba, gelöst. Cesstibtantit aus dem Leshaia Pegmatit (Typlokalität) hat a 10.515(2) Å, Raumgruppe $Fd3m$, die Zusammensetzung $Cs_{0.31}(Sb_{0.57}Na_{0.31}Pb_{0.02}Bi_{0.01})_{\Sigma 0.91}(Ta_{1.88}Nb_{0.12})_{\Sigma 2} \cdot (O_{5.69}OH, F_{0.31})_{\Sigma 6}(OH, F)_{0.69}$, Z 8; die Struktur wurde auf R 3.8, wR 4.3% verfeinert unter Benützung von 96 beobachteten Reflexen. Cesstibtantit vom Tanco Pegmatit hat

a 10.496(1) Å, Raumgruppe $Fd3m$, die Zusammensetzung $(Cs_{0.22}K_{0.01})_{\Sigma 0.23}(Na_{0.45}\cdot Sb_{0.39}Pb_{0.14}Ca_{0.06}Bi_{0.02})_{\Sigma 1.06}(Ta_{1.95}Nb_{0.05})_{\Sigma 2}(O_{5.78}OH, F_{0.22})_{\Sigma 6}(OH, F)_{0.55}$, Z 8; seine Struktur wurde auf R 3.9 wR 3.7% auf der Basis von 104 beobachteten Reflexen verfeinert. Cesstibtantit unterscheidet sich von normalen Pyrochloren insofern, als er signifikante Mengen von sehr großen Kationen, wie z.B. Cs enthält. Da diese Kationen zu groß sind ($^{VIII}r > 1.60$ Å) für eine konventionelle [8]-koordinierte A Stelle, nehmen sie die [18]-koordinierten ϕ Positionen ein, welche normalerweise monovalente Anionen enthalten. Natürliche Cesstibtantitproben sind nicht ideal insofern als sowohl Cs als auch monovalente Anionen in der ϕ Position vorkommen. Somit ist Cesstibtantit intermediär zu den normalen Pyrochloren (mit nur monovalenten Anionen auf der ϕ Position) und den inversen Pyrochloren (mit ausschließlichen großen Kationen an der ϕ Position).

Introduction

Cesstibtantite was discovered by *Voloshin* et al. (1981) at the simpsonite-bearing pegmatite at Leshaia, Kola Peninsula, Russia. On the basis of X-ray crystallographic, chemical and physical properties, they proposed that its structure is a derivative of the pyrochlore structure, and that it has the ideal formula $(Cs, Na)SbTa_4O_{12}$. A summary of data for type cesstibtantite is given in Table 1.

Cesstibtantite has since been found at three other localities: Mt. Holland, W. Australia (*Nickel* and *Robinson*, 1985), the Tanco pegmatite, Manitoba (*Ercit* et al., 1985), and the Dobrá Voda pegmatite, Czechoslovakia (*M. Novak*, pers. comm.). Because of some important differences between these cesstibtantite samples and the description of the type material, we decided to re-examine the species. The properties of type cesstibtantite proved to be more similar to those of the other samples than was initially inferred.

Cesstibtantite is similar to members of the microlite subgroup of the pyrochlore group (*Hogarth*, 1977). It differs in one important regard: its structure is intermediate to the pyrochlore structure and a structure type known to inorganic chemists as the inverse pyrochlore structure. The present paper documents our current understanding of cesstibtantite and serves as an introduction of the inverse pyrochlores to the geological community.

Experimental

Electron Microprobe Analyses

Wavelength-dispersion (WD) electron-microprobe analyses of the Tanco samples were done at the University of Manitoba; WD analyses of the Dobrá Voda samples

Table 1. *Summary of data for type cesstibtantite*

Ideal formula: $(Cs, Na)SbTa_4O_{12}$, $Z = 4$
Symmetry: Cubic, $a = 10.526(5)$ Å
Optics: Isotropic, $n > 1.8$. Colourless to grey, transparent.
Density: obs. = 6.4–6.6 g/cm^3, calc. = 6.49 g/cm^3
Hardness: VHN = 670–780 (100 g load)
Strongest diffraction lines (d, I): 3.17 (9), 3.04 (10), 1.860 (10), 1.587 (10), 1.370 (9), 1.017 (9), 1.012 (10)

were done at the Canadian Museum of Nature. Analysis at the University of Manitoba involved a MAC 5 electron microprobe operating at 20 kV and 40 nA (measured on brass), collection time 10s per element, and a point-focus beam. Reduction of the intensity data was done with a revised version of the EMPADR VII program (*Rucklidge* and *Gasparrini*, 1969). Analysis at the Canadian Museum of Nature involved a JEOL 733 electron microprobe using Tracor Northern 5500 and 5600 automation; operating conditions were 15 kV, 25 nA beam current, 10 μm beam diameter. For these analyses, data were collected for 25 s or 0.5% precision (1σ level), whichever was attained first. Reduction of these intensity data was done with a conventional ZAF routine in the Tracor Northern TASK series of programs.

Energy-dispersion (ED) microprobe analyses of the Leshaia sample were done at the University of Manitoba. The X-ray spectra were collected with a MAC 5 electron microprobe using a Kevex Micro-X 7000 spectrometer. Spectra were collected for 200 live seconds with an operating voltage of 15 kV and a sample current of 5 nA (measured on synthetic fayalite), and were corrected for both current and voltage drift. Some line overlaps such as Ta$M\delta$ and Ta$M\eta$ on Nb$L\alpha$ were dealt with by non-iterative spectral stripping techniques involving library spectra of individual elements taken from standards with matrices similar to the samples. Other line overlaps such as Ca$K\alpha$, β — Sb$L\alpha$, β — Cs$L\alpha$, β interference had to be dealt with by iterative stripping techniques, again involving library spectra. Data were reduced with Kevex software using the MAGIC V program (*Colby*, 1980).

For the analyses done at the University of Manitoba, the standards were microlite (Ta$L\alpha$, $M\alpha$, Ca$K\alpha$, Na$K\alpha$), pollucite (Cs$L\alpha$), stibiotantalite (Sb$L\alpha$, Bi$M\alpha$, Nb$L\alpha$), $CoNb_2O_6$ (Nb$L\alpha$), PbTe (Pb$M\alpha$), cassiterite (Sn$L\alpha$) and orthoclase (K$K\alpha$). For ED analyses, $CoNb_2O_6$ was used as the Nb standard, and the Ta$M\alpha$ line was used; for WD analyses, stibiotantalite was used for Nb, and the Ta$L\alpha$ line was used. For the analyses done at the Canadian Museum of Nature, the standards were $NiTa_2O_6$ (Ta$M\alpha$), synthetic manganocolumbite (Nb$L\alpha$), microlite (Ca$K\alpha$, Na$K\alpha$), pollucite (Cs$L\alpha$), stibiotantalite (Sb$L\alpha$, Bi$M\alpha$), crocoite (Pb$M\alpha$), sanidine (K$K\alpha$), almandine (Fe$K\alpha$) and $CoWO_4$ (W$M\alpha$).

X-Ray Diffraction Experiments

Powder X-ray diffraction work was done with a 114.6 mm diameter Gandolfi camera using Ni-filtered Cu$K\alpha$ radiation. All films were corrected for shrinkage. Indexing and refinement of unit-cell parameters were done with the CELREF program of *Appleman* and *Evans* (1973). For single-crystal diffraction experiments, Charles Supper Co. precession cameras with Zr-filtered Mo$K\alpha$ radiation were used.

Intensity data for the structure analyses were collected with a Nicolet *R*3*m* four-circle diffractometer, using the experimental method of *Ercit* et al. (1986). Because of the intimate association of other Ta-oxide minerals with the cesstibtantite, it was necessary to pluck confirmed cesstibtantite crystals from polished-section and thin-section mounts for both samples used in the experiments. These samples were chemically analyzed prior to their extraction, so that the exact composition of each crystal used in the intensity data collection was known. The Leshaia crystal fragment was plucked from a polished section mount, and was hand-rounded

Table 2. *Miscellaneous data for structure refinements*

KO-1	*SMP-6*
a: 10.515(2) Å	a: 10.496(1) Å
Space group: $Fd3m$	Space group: $Fd3m$
Crystal size: 0.04 × 0.06 × 0.09 mm	Crystal size: 0.03 × 0.12 × 0.13 mm
Crystal shape: tabular, rounded	Crystal shape: $(11, \bar{4}, 8)$ plate
μ (Mo$K\alpha$): 400 cm^{-1}	μ (Mo$K\alpha$): 460 cm^{-1}
Total no. of $\|F_O\|$: 108	Total no. of $\|F_O\|$: 106
No. of $\|F_O\| > 3\sigma$: 96	No. of $\|F_O\| > 3\sigma$: 104
Final R (obs): 3.8%	Final R (obs): 3.9%
Final wR (obs): 4.3%	Final wR (obs): 3.7%
$R = \Sigma(\|F_O\| - \|F_C\|)/\Sigma\|F_O\|$, $wR = [\Sigma w(\|F_O\| - \|F_C\|)^2/\Sigma w\|F_O\|^2]^{1/2}$, $w = 1$	

to an ellipsoid. The Tanco sample was extracted from a thin section, and necessarily had the shape of a plate. The plate was approximately indexed by means of precession photography, and later the index was refined by minimizing the merging R for the ψ-scan dataset (27.1% before correction, 4.2% after correction).

For both crystals, one octant of reciprocal space was collected to a maximum $\sin\theta/\lambda$ of 0.7035, and the data were merged to give the numbers of unique reflections shown in Table 2. The data were empirically corrected for absorption (using the ψ-scan technique), and were corrected for $L \cdot p$ and background effects using the SHELXTL package of programs. A reflection was considered observed if its magnitude exceeded three times its standard deviation; application of this criterion resulted in the numbers of observed reflections given in Table 2.

Physical and Optical Properties

Cesstibtantite is colourless to grey to yellow-orange to black, and ranges in opacity from transparent to translucent; the lustre ranges from vitreous to adamantine. Cesstibtantite fluoresces yellow-orange to orange under long-wave UV light. It is brittle with a hardness of about 5. *Voloshin* et al. (1981) report a range of densities from 6.4 to 6.6 g/cm^3 for the type sample; all other samples are too small and too few in number for density determinations.

Optical data are available only for the type sample and for cesstibtantite from the Tanco pegmatite. Type cesstibtantite is reported to be isotropic with a mean index of refraction greater than 1.8 (*Voloshin* et al., 1981). Cesstibtantite from the Tanco pegmatite is not always isotropic; in thin section, some crystals are anisotropic with a weak birefringence (first-order grey). Anisotropic crystals have vermiform optical domains; to date, no optically continuous anisotropic crystals have been found.

At all localities, crystals of cesstibtantite are very small, typically 0.1 to 0.5 mm in diameter. At the Leshaia pegmatite, cesstibtantite occurs as irregularly-shaped aggregates along simpsonite-stibiotantalite grain boundaries, in fractures in these

minerals, and in fine intergrowths with microlite. At the Tanco pegmatite, cesstibtantite occurs as isolated crystals or as overgrowths on antimonian and uranian varieties of microlite. In both occurrences at Tanco, the dominant morphology is cuboctahedral. At both Mt. Holland and at the Dobrá Voda pegmatite, cesstibtantite occurs as an alteration product of probable stibiotantalite, and is thus irregular in shape.

X-Ray Crystallography

X-ray powder diffraction data were collected on cesstibtantite samples from the Leshaia pegmatite and the Tanco pegmatite (Table 3). Both diffraction patterns can

Table 3. *Powder diffraction data for cesstibtantite*

hkl	KO-1		SMP-6	
	d	*I*	*d*	*I*
111	6.07	8	6.07	8
311	3.17	9	3.16	9
222	3.03	10	3.03	10
400	2.632	7	2.625	8
331	2.417	1	2.406	1
511, 333	2.026	7	2.021	6
440	1.861	9	1.856	9
531	1.776	4	1.774	3
533	1.606	2	1.600	1
622	1.586	8	1.582	9
444	1.518	2	1.514	2
711, 551	1.472	4	1.470	3
731, 553	1.370	6	1.367	4
800	1.315	1	1.311	3
751, 555	1.214	1	1.212	1
662	1.206	3	1.204	3
840	1.177	3	1.175	3
911, 753	1.155	2	1.154	1
931	1.1017	2	1.1005	1
844	1.0734	2	1.0713	2
933, 771	1.0565	<1		
951, 773	1.0168	1	1.0151	2
1022, 666	1.0123	4	1.0102	4
a (Å)	10.522(3)		10.497(1)	

114.6 mm dia. Gandolfi camera, Ni-filtered CuKα radiation. Corrected for shrinkage.
KO-1: Leshaia, Kola Peninsula, USSR.
SMP-6: Tanco pegmatite, Manitoba

Table 4. *Reinterpretation of the type diffraction pattern for cesstibtantite*

I	1	2	3	*I*	1	2	3
6	6.06	6.06	6.06	1*d*	1.197		1.197
9	3.17	3.17	3.17	6	1.177	1.177	
10	3.04	3.04	3.04	3	1.176 *		
7	2.631	2.631	2.631	6	1.156	1.156	
3	2.415	2.415		3	1.155 *		
8	2.024	2.024	2.024	7	1.1032	1.1032	
10	1.860	1.860		4	1.1027 *		
1	1.846		1.846	8	1.0738	1.0738	
5	1.779	1.779		5	1.0738 *		
1	1.662	1.662		1	1.0644		1.0644
5	1.605	1.605		1	1.0644 **		
10	1.587	1.587		6	1.0572	1.0572	
1	1.574		1.574	3	1.0571 *		
3	1.520	1.520		1*d*	1.0460	1.0460	1.0460
8	1.474	1.474		1*d*	1.0258 ?		
1	1.461		1.461	9	1.0173	1.0173	
9	1.370	1.370		5	1.0169 *		
1*d*	1.358		1.358	10	1.0123	1.0123	
6	1.317	1.317		7	1.0121 *		
1*d*	1.305		1.305	2	1.0035		1.0035
3	1.287	1.287		1	1.0035 **		
7	1.216	1.216		3	0.9840 ?		
3	1.216 *			5	0.9811	0.9811	
8	1.208	1.208		3	0.9810 *		
3	1.208 *						

1. Type pattern (*Voloshin et al.*, 1981). *2.* Cesstibtantite component: $a = 10.525(1)$ Å. *3.* Microlite component: $a = 10.436(2)$ Å.
KEY: *d*—diffuse, *—Fe$K\alpha_2$ component of cesstibtantite, **—Fe$K\alpha_2$ component of microlite, ?—unexplained contaminant

be completely indexed on a cubic cell with $a \simeq 10.5$ Å, space group $Fd3m$. The refined unit cell parameters (Table 3) show that the cell of cesstibtantite from Leshaia is slightly larger than that of the Tanco specimen.

Powder diffraction data for type cesstibtantite are given in Table 4. The pattern reported by *Voloshin* et al. (1981) is different from the ones obtained in the present study: In the type pattern, (1) there are reflections which violate the F-centering—*e.g.* at 1.846 Å, (2) several high-angle reflections are "split"—*e.g.* the 1.156 Å reflection seems to be split into two reflections at 1.156 and 1.155 Å, and (3) there are several reflections with $I = 10$. Regarding the first point, the reflections which violate the F-centering can all be indexed and refined on a cubic F-centered cell ($Fd3m$) with $a = 10.436(2)$ Å. This is exactly the correct symmetry and metricity for the unit cell of common microlite, $(Na, Ca)_{\Sigma 2}Ta_2O_6(OH, F)$. *Voloshin* et al. (1981) document microlite and cesstibtantite intergrowths at the type occurrence; it seems very likely that all reflections which fit this cubic cell are due to microlite contamination. Regarding point (2), without exception, all of the higher-*d* components of the "split"

Table 5. *Cesstibtantite*: "*forbidden*" *reflections*

($I/I_0 \leq 1$)									
244,	446,	248,	468,	288,	688,	44$\underline{1}$0,	48$\underline{1}$0,	24$\underline{1}$2,	28$\underline{1}$2

reflections can be indexed on the cell that we obtained for cesstibtantite from Leshaia (Table 3). The components with lower d values are consistently one-half as intense as their higher-d counterparts, and fall exactly in the right location for a misidentified $K\alpha_2$ component (assuming Fe$K\alpha$ radiation was used). The consistency of both observations leads us to conclude that these "split" reflections probably result from unrecognized $K\alpha_1 - K\alpha_2$ resolution. The different d values reported for each component (Table 4) would thus result from the use of incorrect values of λ in Bragg's equation for the weaker, $K\alpha_2$ component of each doublet. Because *Voloshin* et al. (1981) do not report the type or wavelength of radiation used in their experiments, this probability cannot be explored further. The explanation of point (3) is relatively straight-forward. An abundance in any X-ray diffraction pattern of reflections with $I = 10$ strongly suggests that the maximum optical density of the X-ray film was exceeded; *i.e.*, the type pattern was overexposed.

Precession photographs were taken of cesstibtantite samples from Leshaia and the Tanco pegmatite (0 to 3rd levels, Mo$K\alpha$ radiation). All intensity relationships conform completely to $Fd3m$ symmetry, and there are no metric deviations from cubic symmetry; this suggests that cesstibtantite has the pyrochlore structure. However, cesstibtantite samples from both localities were found to have some weak reflections in their precession photographs which are not shown by normal pyrochlores (Table 5). Although these reflections do not violate $Fd3m$ symmetry, they transgress extinction conditions for the pyrochlore structure—all atoms in the pyrochlore structure are at special positions, and thus the X-ray diffraction properties of the pyrochlore structure follow tighter extinction conditions than $Fd3m$ imposes.

Chemistry

Electron-microprobe analyses of cesstibtantite samples are given in Table 6. The average analysis of *Voloshin* et al. (1981) for type cesstibtantite agrees well with our analyses for off-type material from the same locality. The analyses of samples from other localities show that (1) Ta ⇄ Nb isomorphism can be extensive—the sample from Dobrá Voda has 30% of its Ta replaced by Nb, (2) extensive Sb ⇄ Pb substitution occurs; the Pb:Sb ratio ranges from 0 (Dobrá Voda) to 0.61 (Tanco), (3) Cs contents are not highly variable, (4) Na contents are highly variable and are not strongly correlated with other parameters or combinations of parameters.

Voloshin et al. (1981) have suggested formula calculation on a basis of 12 oxygen atoms. They observed a nearly 1:1:4:12 ratio of (Cs + Na + Ca):(Sb + Bi + Pb):(Ta + Nb):O for their analyses and proposed that cesstibtantite has the structural formula $AA'B_4O_{12}$ where A = Cs, Na, Ca, (K); A' = Sb^{3+}, Bi, Pb, (Sn^{2+}, Mn, Fe); and B = Ta, Nb, (W) (quantities in parentheses are inferences made by the present authors). Actual ratios on a basis of 12(O) are:

Table 6. *Electron microprobe analyses of cesstibtantite*

	1	2	3	4	5	6
Na_2O (wt%)	1.3	1.7	2.4	2.1	2.2	2.2
K_2O	----	0.0	0.05	0.0	0.05	----
Cs_2O	7.3	7.4	5.4	5.3	7.0	6.5
CaO	0.1	----	0.6	0.6	0.2	----
MnO	----	----	----	----	0.0	----
FeO	----	----	----	----	0.1	0.1
SnO	----	----	0.1	0.0	0.0	----
PbO	1.6	0.8	5.3	8.0	0.0	----
Sb_2O_3	13.6	14.2	9.7	8.5	14.8	17.0
Bi_2O_3	0.7	0.3	0.6	1.0	0.0	----
Nb_2O_5	2.3	2.8	1.2	0.8	14.0	5.1
Ta_2O_5	72.0	70.8	72.5	70.6	56.2	65.3
WO_3	----	----	----	----	0.3	----
F	----	----	----	----	0.0	----
	98.9	97.9	97.8	96.9	94.9	96.2
	Cations per 2 (Ta, Nb, W)					
K	----	0.000	0.007	0.000	0.006	----
Cs	0.300	0.308	0.219	0.233	0.280	0.276
Na	0.244	0.312	0.451	0.417	0.395	0.425
Ca	0.014	0.000	0.063	0.063	0.019	----
Fe	----	----	----	----	0.010	0.008
Sn^{2+}	----	0.000	0.009	0.000	0.000	----
Pb	0.042	0.021	0.141	0.222	0.000	----
Sb	0.543	0.571	0.393	0.358	0.560	0.699
Bi	0.017	0.007	0.016	0.026	0.000	----
Nb	0.102	0.124	0.052	0.035	0.583	0.230
Ta	1.898	1.876	1.948	1.965	1.409	1.770
W	----	----	----	----	0.008	----
	3.130	3.219	3.299	3.319	3.270	3.408
O (eff)*	6.168	6.202	6.160	6.185	6.213	6.407

1. Leshaia, USSR. Average from *Voloshin* et al. (1981), 2. Leshaia, USSR, Sample KO-1; average of 2 analyses, 3. Tanco pegmatite, Manitoba. Sample SMP-6; average of 2 analyses, 4. Tanco pegmatite, Manitoba. Sample TSE-51B; average of 2 analyses, 5. Dobrá Voda, Czechoslovakia. Average of 2 analyses, 6. Mt. Holland, W. Australia. *Nickel* and *Robinson* (1985). "----": not sought; "0.0": not detected; *: for charge balance

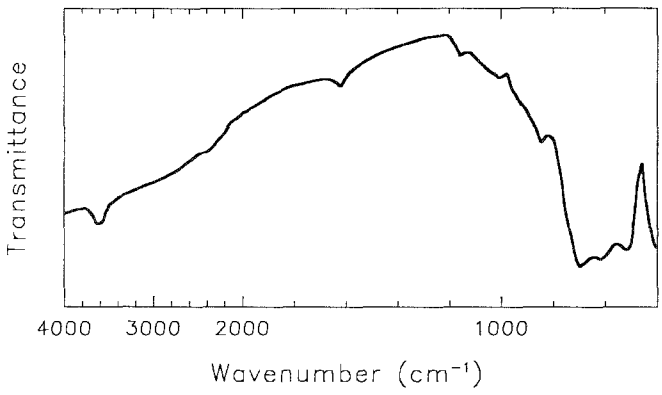

Fig. 1. Infrared spectrum of type cesstibtantite (after *Voloshin* et al., 1981)

1.09:1.18:3.89:12 (Leshaia, *Voloshin* et al., 1981)
1.22:1.16:3.87:12 (Leshaia, present study, sample KO-3)
1.46:1.08:3.89:12 (Tanco, present study, sample SMP-6)
1.39:1.18:3.88:12 (Tanco, present study, sample SMP-51B)
1.35:1.10:3.86:12 (Dobrá Voda, present study)
1.31:1.33:3.75:12 (Mt. Holland, *Nickel* and *Robinson*, 1985)

All analyses are non ideal, often quite significantly: our re-analysis of cesstibtantite from Leshaia shows a 22% surplus at the A site which is exceeded by all other analyses or samples; the type analysis shows an 18% surplus at the inferred *A'* site, for which the Mt. Holland sample shows a 33% surplus; all samples show a deficit at the inferred *B* site of 3 to 6%. Some of the smaller deviations might be explained as due to ZAF errors; however, deviations in the neighborhood of 30 to 50% and wide ranges in the degree of deviation clearly indicate a problem with the model. Cesstibtantite does not show $AA'B_4O_{12}$ stoichiometry.

The infrared spectrum of type cesstibtantite from Leshaia (*Voloshin* et al., 1981) is reproduced in Figure 1. The absorptions at 1625 cm^{-1} and 3625 cm^{-1} indicate the presence of H_2O and OH, the former of uncertain origin and role because of the absence of any information on sample preparation. Quite clearly, a basis of 12(O) is not suitable for formula calculation if appreciable OH is present. Furthermore, *Voloshin* et al. (1981) do not indicate whether F was sought in the analyses; because microlites are often rich in F (*Eid* and *von Knorring*, 1981), and because type cesstibtantite is structurally similar to microlite, which it replaces, the presence of F is a strong possibility.

As with pyrochlore-group minerals, when OH + F contents are not known, formula contents are best calculated by normalizing on the *B*-site sum. This is the approach taken in Table 6, wherein we report atomic proportions for cesstibtantite samples by normalizing on 2 (Ta + Nb + W), *i.e.* by analogy with the pyrochlore-group minerals. For this calculation procedure, the cesstibtantite compositions show effective oxygen numbers (calculated for charge balance, in absence of data on OH and F) in excess of 6 anions per formula unit. It is tempting to calculate maximum H_2O by assigning two times the excess to be OH by analogy with pyrochlore-group minerals, but structure determinations are needed before this can be done with any confidence.

Structure Analysis and Refinement

With the intention of testing the validity of the structural model of *Voloshin* et al. (1981) for cesstibtantite, and to eliminate the ambiguities discussed in the previous section, structure analyses were done for cesstibtantite samples from the pegmatite at Leshaia (sample KO-3) and the Tanco pegmatite (sample SMP-6). The program SHELXTL was used for all calculations.

Unit-cell refinement based on the subset of reflections used in centering the crystal gave the following *unconstrained* unit-cell parameters. (1) Tanco sample: $a = 10.500(2)$, $b = 10.497(2)$, $c = 10.494(2)$ Å, $\alpha = 90.05(2)$, $\beta = 89.96(2)$, $\gamma = 90.01(2)°$; (2) Leshaia sample: $a = 10.519(5)$, $b = 10.514(4)$, $c = 10.511(3)$ Å, $\alpha = 89.98(3)$, $\beta = 89.99(3)$, $\gamma = 90.06(3)°$. The results of both unconstrained refinements indicate that the samples are metrically cubic. Unit-cell refinements with cubic constraints gave the cell edges reported in Table 2; both results are in excellent agreement with the cell edges refined from powder data (Table 3).

Because of the strong similarities between the X-ray diffraction properties of cesstibtantite and the pyrochlores, the pyrochlore structure was used as a starting model for the analysis of the cesstibtantite structure. The starting model had all Na, Cs, Sb, Bi, Sn, Pb and Ca at the pyrochlore *A*-cation site, and had all Ta and Nb at the *B*-cation site. The O-site occupancy was fixed at 1; initially the ϕ-site was set at one-half occupancy. Isotropic temperature factors were refined for each site, and the total occupancy of the ϕ and *A* sites were refined. Refinement converged at $R = 5.6\%$, $wR = 5.4\%$ for the Tanco sample and $R = 6.5\%$, $wR = 7.1\%$ for the Leshaia sample. Despite the reasonable *R* indices, both models had the following undesirable features:

1. The *A* site had large values of *U*: 0.074 Å^2 for the Tanco sample and 0.186 Å^2 for the Leshaia sample. In addition, the *A*-site occupancy refined to 20% (Tanco) and 25% (Leshaia), significantly lower than expected from microprobe analyses.
2. The occupancy of the ϕ site refined to 2 (Tanco) and 2.5 (Leshaia) times the allowable maximum (8 atoms per unit cell), assuming oxygen to be the only occupant. Furthermore, the oxygen curve did not model scattering about the site well; difference-Fourier maps showed a single large residual maximum (3 e/Å^3 for the Tanco sample and 6 e/Å^3 for the Leshaia sample) at the ϕ site.

These features indicated that there was too little scattering at the *A* site and too much scattering at the ϕ site to be accounted for by a normal pyrochlore model. On the basis of arguments presented in the next subsection, the *A*-site constituents Cs and K were transferred to the ϕ site and the data were re-refined. The *B* and *O* ions were modelled as vibrating anisotropically; ϕ is constrained by symmetry to vibrate isotropically. At this stage, the temperature factor for the *A* cation was still large: $U = 0.072$ (Tanco), 0.168 Å^2 (Leshaia). A $\Delta(A)$ difference-Fourier map showed an elongate ellipsoidal maximum for the Tanco sample, and a dumbell-shaped maximum for the Leshaia sample, indicating that the *A* cations are positionally disordered. The observed electron-density distributions indicated that the A cations actually occupy a 96*g* position near the ideal 16*d* position, producing a sixfold increase in site multiplicity, which is necessarily accompanied by a sixfold decrease in the site occupancy. Consequently, positional constraints for the *A* site were

Table 7. *Atomic positional and thermal parameters for cesstibtantite samples*

	Parameter	KO-1	SMP-6
A	*x*, *y*	0.518(1)	0.513(2)
	z	0.455(1)	0.471(2)
	U	150*	150*
B	*x*, *y*, *z*	0	0
	U_{11}, U_{22}, U_{33}	202(5)	98(4)
	U_{12}, U_{13}, U_{23}	−40(4)	−26(3)
O	*x*	0.314(2)	0.311(1)
	y, *z*	1/8	1/8
	U_{11}	212(82)	162(74)
	U_{22}, U_{33}	233(50)	255(48)
	U_{12}, U_{13}	0	0
	U_{23}	43(67)	81(66)
ϕ	*x*, *y*, *z*	3/8	3/8
	U	580(45)	370(37)

All *U* values are $Å^2 \times 10^4$. *: fixed value

Table 8. *Bond lengths (Å) for cesstibtantite samples*

	KO-1	SMP-6
A Polyhedron		
$A - O \times 2$	2.47(1)	2.55(1)
$- O \times 2$	3.01(1)	2.91(1)
$- O \times 1$	2.18(2)	2.37(3)
$- O \times 1$	3.22(2)	3.06(3)
$- \phi \times 1$	2.29(2)	2.28(3)
$- \phi \times 1$	2.39(2)	2.32(3)
$\langle A - O \rangle$	2.63	2.62
A' Polyhedron		
$A' - O \times 6$	3.27(2)	3.29(2)
$- O \times 12$	3.772(3)	3.771(3)
$\langle A' - O \rangle$	3.605	3.611
B Polyhedron		
$B - O \times 6$	1.978(5)	1.963(5)

Table 9. *Polyhedral edge lengths (Å) and angles (°) for cesstibtantite samples*

	KO-1		SMP-6	
A' Polyhedron				
O – O × 24	2.78(1),	45.8(0)	2.79(1),	45.9(0)
– O × 12	4.63(3),	75.5(4)	4.66(2),	76.3(3)
– O × 12	2.81(3),	43.8(4)	2.76(2),	43.0(4)
⟨O – O⟩	3.25		3.25	
⟨O – *A'* – O⟩		52.7		52.8
A Polyhedron				
O – O × 2	2.78(1),	60.1(2)	2.79(1),	61.0(1)
– O × 2	2.78(1),	73.2(4)	2.79(1),	68.9(6)
– O × 2	2.78(1),	52.9(3)	2.79(1),	52.6(4)
– ϕ × 2	3.27(2),	86.8(5)	3.30(1),	85.7(7)
– ϕ × 2	3.27(2),	73.5(4)	3.30(1),	77.1(6)
– ϕ × 1	3.27(2),	91.2(8)	3.30(1),	89.3(11)
– ϕ × 1	3.27(2),	70.4(5)	3.30(1),	74.5(9)
⟨O – O, ϕ⟩	3.03		3.05	
⟨O – *A'* – O, ϕ⟩		71.2		71.2
B Polyhedron				
O – O × 6	2.78(1),	89.5(6)	2.79(1),	89.3(6)
– O × 6	2.81(3),	90.5(6)	2.76(1),	90.7(6)
⟨O – O⟩	2.80		2.78	
⟨O – *B* – O⟩		90.0		90.0

relaxed to conform with the symmetry of the 96*g* position, and the positional parameters for the *A* cation were refined. Because of high covariance between the positional parameters and the temperature factor for the *A* cation, the temperature factor was fixed at a value of $U = 0.015$ Å^2, comparable to $U(A)$ for microlites (*Ercit*, 1986).

An attempt was made to refine the anion occupancy of the ϕ site while using microprobe-constrained cation occupancies. Refinement converged at over twice the calculated number of effective oxygen atoms for the site (*i.e.* for charge balance assuming O^{2-} as the sole anion), indicating that the anion content of the ϕ site is all monovalent, *i.e.* all OH, F. The anion content of the ϕ site was suitably constrained in later stages of the refinement to reflect this conclusion.

In the final stages of refinement, microprobe-constrained occupancies were used for the various sites. Refinement converged at $R = 3.9$, $wR = 3.7\%$ for the Tanco sample, and $R = 3.8$, $wR = 4.3\%$ for the Leshaia sample. Final positional and thermal parameters are given in Table 7, selected bond lengths in Table 8, and polyhedral edge-lengths and angles in Table 9. Observed and calculated structure factors are available from the authors upon request.

Normal and Inverse Pyrochlores and the Cesstibtantite Structure

As described in previous sections, cesstibtantite is similar to the pyrochlore group minerals. However, there are several features of its chemistry and structure shown by no other pyrochlore-group mineral; they warrant further discussion here.

The Normal Pyrochlores

The general formula of the pyrochlore-group minerals (*Hogarth*, 1977) is:

$$A_{2-m}B_2O_6\phi_{1-n}\cdot pH_2O \qquad (Z = 8)$$

A ranges from monovalent to trivalent. The most typical *A* cations are Na and Ca; less common *A* cations are Ba, Bi, K, Pb, REE, Sb^{3+}, Sn^{2+}, Sr, Th, U, Y and Zr. The smaller *B* cations are either quadrivalent or pentavalent. Typical *B* cations are Nb, Ta and Ti; atypical ones such as Sn^{4+} and Fe^{3+} occur in trace to minor quantities. In the IMA-recommended formula given here, a distinction is made between the six oxygen atoms which coordinate each *B* cation, and the other anion which is bonded only to the *A* cation. This anion, here denoted ϕ, can be OH, F or O. Some pyrochlore-group minerals also contain structural H_2O groups; the upper limit is not well-established, but is in the neighbourhood of one molecule per formula unit.

Vacancies, indicated in the formula by the subscripts *m* and *n*, can occur at the *A* site or the ϕ site; observed ranges for natural pyrochlores are: $m = 0 \rightarrow 1.75$, $n = 0 \rightarrow 1$. Structure refinements of natural and synthetic pyrochlores show that the *B* site is always fully occupied. Although the IMA-recommended formula for pyrochlore-group minerals indicates that the O site is also fully occupied, some recent refinements of synthetic pyrochlores of unusual composition (*Groult* et al., 1982) show that it is possible to have minor proportions of vacancies at this site. Consequently, the only acceptable basis for formula calculation is normalization of the *B* sum to 2 cations per formula unit.

The pyrochlore structure is a derivative of the fluorite structure, with ordered vacancies. The fluorite structure consists of cubic cation coordination polyhedra, such that each edge of each cube is shared with an adjacent cube (Fig. 2a). The *ideal pyrochlore structure* can be conceptually derived from the fluorite structure by replacing one-half of the cubes of the fluorite structure with octahedra. This is done by removing oxygen atoms at two opposing corners of each cube involved. In the structure that results (Fig 2b), *B* cations occur at the centres of the octahedra, and *A* cations occur near the centres of the remaining cubes, coordinated by 6 oxygen atoms and 2 ϕ anions. When present, H_2O groups occur in the vicinity of the ϕ site (*Groult* et al., 1982).

Pyrochlore-group minerals are typically non-ideal; they have incomplete *A*- and ϕ-site occupancies. If these sites were completely vacant, an empty framework of BO_6 octahedra would result (Fig. 2c). This structure is shown by some Ta-W pyrochlores (*Groult* et al., 1982), and is called the *defect pyrochlore structure*. It is surprising that this terminology is not used by the mineralogical community, as virtually all pyrochlore-group minerals have structures which are intermediate to the ideal and defect pyrochlore structures.

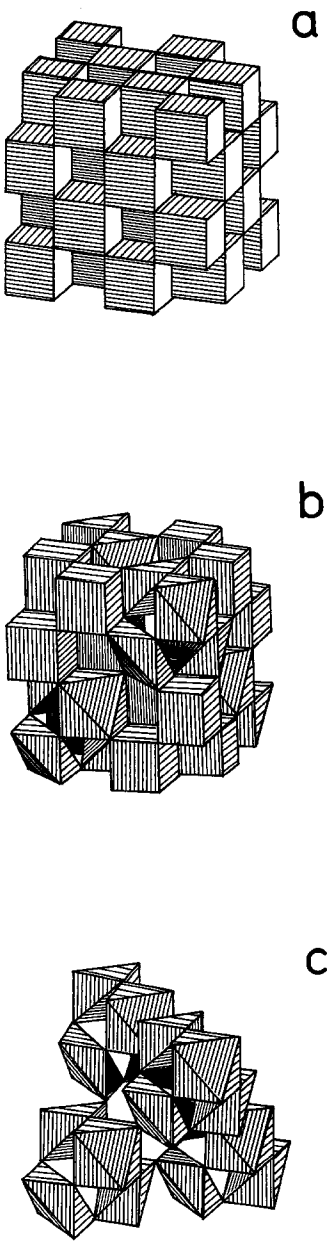

Fig. 2. Polyhedral representations of the fluorite (**a**), ideal pyrochlore (**b**) and defect pyrochlore (**c**) structures. The *ideal pyrochlore structure* can be derived from the fluorite structure by replacing 1/2 of the cubes of the fluorite structure with octahedra. In the resulting structure, the *A*-cation polyhedra are the remaining cubes, the *B*-cation polyhedra are the octahedra. The *defect pyrochlore structure* is derived from the ideal pyrochlore structure by removing all *A*-cation polyhedra, resulting in a framework of *B*-cation octahedra with large cavities

Solid-state chemists refer to the group of all pyrochlores with structures ranging from the ideal to defect types as normal *pyrochlores*; we have adopted this very practical terminology in our discussions here.

The Inverse Pyrochlores

Yet another class of pyrochlores has been recognized by solid-state chemists. Although formally known for 50 years (*Schrewelius*, 1943), widespread recognition of this class emerged only 15 to 20 years ago. These compounds are referred to as the *inverse pyrochlores*, and have the structural formula

$$\square B_2O'_6A'$$

where □ represents a vacancy, A' is a large monovalent cation (typically Cs, Rb or Tl), B is a relatively small tri- to hexavalent cation, and O′ is O, OH or F.

In these compounds, the B cations play the same structural role as do the B cations of the pyrochlore structure; however, both O and monovalent anions occur at what was the O site of the pyrochlore structure, denoted O′ here . The cations which we would normally consider to be A cations, namely Cs, Rb, and Tl, do not occur at the A site of the normal pyrochlore structure. Instead, they occupy what was the ϕ site of the normal pyrochlore structure, and what was the A site remains vacant, hence the symbol "□" in the structural formula.

Some synthetic normal pyrochlores have the general structural formula

$$AB_2O_6\square$$

with half-occupied A sites and completely vacant ϕ sites (*Subramanian et al.*, 1983). Comparison of this formula for a normal pyrochlore to the structural formula given above for the inverse pyrochlores shows that for the inverse pyrochlore structure, the "A" cations and vacancies are *inverted* in terms of their structural roles, hence the nomenclature.

Whether a given A cation adopts a normal or inverse distribution depends upon the radius ratio $A:B$. For B = (Nb, Ta, Ti, W), cations larger than Tl^+ (r = 1.59 Å in [8]-coordination, *Shannon*, 1976) cannot be stabilized at the A site, and reside instead at the ϕ site of the pyrochlore structure (*Fourquet* et al., 1973). Of these cations, only *Cs* is large enough to be properly stabilized at the ϕ site. Smaller cations are positionally disordered about the ideal ϕ-site position along the threefold axis passing through the site, the magnitude of the displacement varying inversely with ionic radius (*Fourquet* et al., 1973).

Cations with [8]-coordinated radii in the range r = 1.50 to 1.60 Å (*i.e.*, K, Tl) can occur at either or both of the ϕ and A sites of the pyrochlore structure (*Fourquet* et al., 1970, *Grins* et al., 1980) depending upon the ratio of the number of A cations to B cations. For $A:B$ = 1:1, the A cations adopt a normal distribution; for

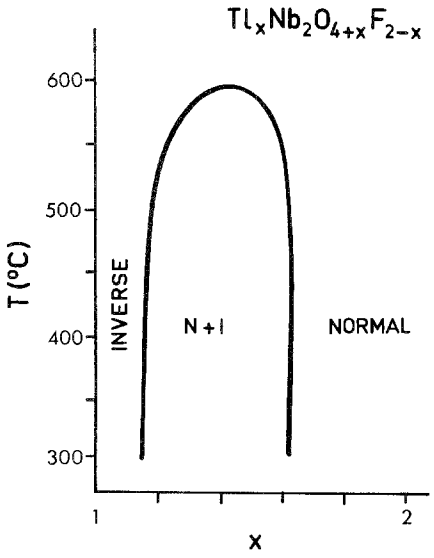

Fig. 3. Compositional-structural variations in Tl pyrochlore (after *English* and *Sleight*, 1980). Although considerable inverse pyrochlore (*I*) is soluble in normal pyrochlore (*N*), the reverse is not true. The large field in the centre of the diagram marks a two-phase region where both phases are stable

$A:B = 1:2$, they take an inverse distribution. Intermediate $A:B$ ratios produce either single phases with A cations at both the A and ϕ sites or two-phase mixtures, depending upon the exact $A:B$ ratio and temperature (Fig. 3). Cesstibtantite is similar to this last group of compounds in that it has A cations at both the A and ϕ sites, yet is dissimilar in that it also has anions at the ϕ-site.

The Cesstibtantite Structure

Figure 4 is a simplification of the environment of the A' (Cs) site of cesstibtantite. The A' site is surrounded by six oxygen atoms, each at a distance of approximately 3.28 Å, and by 12 more oxygens at a distance of approximately 3.77 Å (Fig. 5). These bond lengths are well within the normal range of Cs-O bond lengths for compounds with highly-coordinated Cs polyhedra (*e.g. Oyetola* et al., 1988).

If the A cation in cesstibtantite were located at its ideal position (16*d*, symmetry $\bar{3}$m), there would be four A cations around each ϕ site at a distance of only 2.3 Å (Fig. 4). Instead, positional disorder of the A cation off the $\bar{3}$ axis results in 24 fractionally-occupied A sites about each A' site. Half of these lie closer to the A' site ($A - A' = 2.28$ Å, 2.29 Å for Tanco, Leshaia), half lie farther ($A - A' = 2.32$, 2.39 Å for Tanco, Leshaia) than the ideal A position. It is tempting to suggest that the

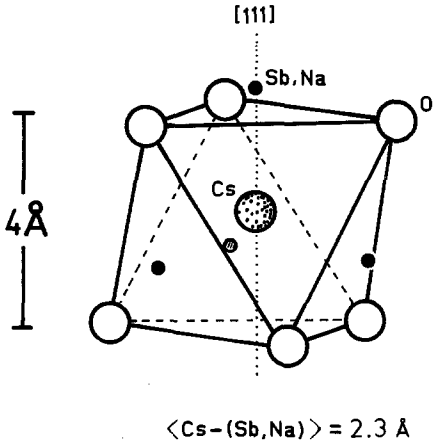

Fig. 4. Idealized first nearest-neighbour environment about the A' cation of the cesstibtantite structure. For simplicity, twelve oxygens (O site) at 3.77 Å from the A' cation are not shown

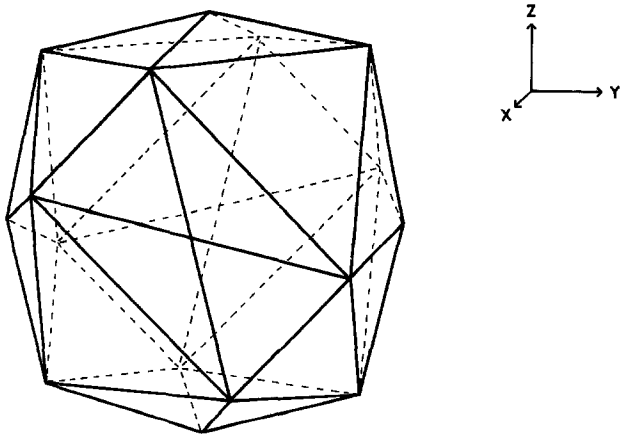

Fig. 5. Coordination polyhedron of the A' cation. The A' cation is 18-coordinated, with 6 oxygens at 3.3 Å and 12 at 3.8 Å, resulting in a coordination polyhedron with 32 faces (distorted trapezohedron with octahedral modifications)

proximity of the A and A' cations is responsible for the positional disorder of the A cations; *i.e.*, that positional disorder is the only way a stable separation between these cations can be obtained. However, as the maximum cation-cation separations resulting from positional disorder are too short to represent stable Cs-Sb separations, this model seems unlikely.

Positional disorder of the A cation is not a phenomenon unique to the inverse pyrochlores. Synthetic normal pyrochlores with the composition $Sn^{2+}{}_{2-x}(M_{2-y}Sn^{4+}{}_y)O_{7-x-y/2}$ where M = Nb, Ta (*Birchall* and *Sleight*, 1975) show anomalous behaviour of the A cation. Here Sn^{2+} is displaced from the 16*d* position toward a 96*g* position with $x = 0.518(1)$ and $z = 0.474(1)$, in a manner identical to the A cation of cesstibtantite. Hence it is possible that positional disorder of the A cation of cesstibtantite is not due to cation-cation repulsion, but rather to some other stimulus.

An important point to consider is that the displacement of the A cation from the ideal 16*d* position is greater for the Leshaia sample than for the Tanco sample (Table 7). In terms of A-cation composition, the Leshaia sample differs most from the Tanco sample in having a higher $Sb^{3+}:Na^+$ ratio; is positional disorder somehow related to Sb^{3+} content? The ideal A-cation site is highly symmetric ($\bar{3}$m symmetry); if Sb^{3+} in cesstibtantite has a stereoactive lone-pair of electrons, then location of the Sb^{3+} at 16*d* would be highly unlikely. In that both Sn^{2+} and Sb^{3+} are typical lone-pair cations, and because the style and magnitude of positional disorder of Sn^{2+} and Sb^{3+} in synthetic Sn-pyrochlore and cesstibtantite, respectively, are nearly identical, it would seem likely that positional disorder of the A cation is due to stereoactivity of lone electron pairs. Because X-ray crystallographic investigations give the average behaviour of the A cation, with increasing content of the lone-pair cation, namely Sb^{3+}, cesstibtantite samples seem to show increasingly greater displacement of the A cation from the $\bar{3}$ axis.

If the above model is correct, then normal pyrochlores with Sb^{3+} as their sole A-site constituent must have similar A-cation behaviour as cesstibtantite. To date, only one structure refinement of a normal Sb^{3+}-pyrochlore has been done: synthetic Sb_6O_{13} (*Stewart* et al., 1972). The formula of this compound is better written as $Sb^{3+}Sb^{5+}{}_2O_{6.5}$ to compare with the structural formula for the pyrochlore group. The compound has the normal pyrochlore structure, with Sb^{5+} at the B site, O at the O and ϕ sites and Sb^{3+} at the A site. The model of *Stewart* et al. (1972) has Sb^{3+} at the ideal position (16*d*); however, the temperature factor (B) of 6.3 Å^2 is clearly unacceptable and compares with $B = 5.8$ Å^2 for the Tanco cesstibtantite before positional disorder was modelled. Thus it would seem that Sb^{3+} in the normal pyrochlore $Sb^{3+}Sb^{5+}O_{6.5}$ behaves similarly to Sb^{3+} in cesstibtantite.

Only one structure analysis has been done on a synthetic inverse pyrochlore with Sb^{3+}: the compound $K_{0.51}Sb^{3+}{}_{0.67}Sb^{5+}{}_2O_{6.26}$ (*Piffard* et al., 1978). This inverse pyrochlore, quite coincidentally, is the only synthetic pyrochlore with non-isochemical A- and A'-site populations, and with cation-anion ϕ-site disorder like cesstibtantite. It has Sb^{5+} at the B site and O at both the O and ϕ sites; however, Sb^{3+} shows positional disorder about the A site, and K shows positional disorder about the A' ($= \phi$) site. The behaviour of Sb^{3+} is identical to that observed for A cations in cesstibtantite: Sb^{3+} fractionally occupies a 96*g* position. The behaviour of K in this pyrochlore is not identical to that of Cs in cesstibtantite; because of its small size, K fractionally occupies both a 32*e* position and a 96*g* position about the

ideal 8*b* position. Although the study of this synthetic, mixed normal-inverse pyrochlore adds no further insights into the crystal chemistry of mixed normal-inverse pyrochlores, it does confirm the assignment of Sb^{3+} to the 96*g* position, and confirms the possibility of A' cation versus ϕ anion disorder.

Other possible candidates for non-ideal A-cation behaviour are Pb^{2+} and Bi^{3+} pyrochlores. The structure of the normal pyrochlore $Pb^{2+}{}_{1.5}Nb_2O_{6.5}$ (synthetic plumbopyrochlore) has been refined (*Bernotat-Wulf* and *Hoffmann*, 1982). The Pb^{2+} cation occurs at the ideal 16*d* position, and has a normal isotropic displacement parameter: $B = 1.71(3)$ Å. The extra electron pair of Pb^{2+} would seem to be stereochemically inactive in pyrochlores. As regards the Bi^{3+} pyrochlores, unfortunately the only structure refinements to date (*Jeanne* et al., 1974) did not involve refinement of individual displacement factors of the atoms, and assumed ideal behaviour for Bi^{3+}; thus no data are available for the bonding tendencies of Bi^{3+} in pyrochlores.

The following set of points lists the important features of the cesstibtantite structure:

1. Cesstibtantite is a pyrochlore with mixed inverse-normal character. All compositions have anions in excess of 6 per formula unit. By analogy with the inverse pyrochlore $CsNb_2O_5F$ (*Fourquet* et al., 1973), if there is 1 (OH + F) at the O site per Cs atom at the A' site, then for local charge balance there are 0.23 *effective* oxygen atoms p.f.u. at the ϕ site for the Tanco sample and 0.31 *effective* oxygen atoms p.f.u. at the ϕ site for the Leshaia sample. Structure refinement showed the ϕ-site occupancy to be in excess of twice these values for both samples, hence monovalent anions are more probable for this site. On this basis, there would be 1.5 wt.% and 1.2 wt% H_2O for the Leshaia (KO-1) and Tanco (SMP-6) samples, respectively, assuming all ϕ^- to be OH. Both figures compare well with the observed analysis deficits of Table 6.
2. A very open-ended structural formula for cesstibtantite is:

$$A_{2-m}B_2O'_6(\phi, A')_{1-n}$$

where A = Na, Sb^{3+}, Pb^{2+}, Bi^{3+}, Ca, Sn^{2+}
B = Ta, Nb
O′ = O, OH, F
ϕ = OH, F
A' = Cs, K

More rigid formulations can be written for ideal mixtures of normal and inverse pyrochlores; for example, from stereochemical considerations (Fig. 4), if there is no short-range ordering of cations and vacancies at the A site, the following limits apply: as Cs → 0, $m \rightarrow 4$(Cs) and as Cs → 1 (upper limit), $m \rightarrow 2$(Cs). For the samples used in the structural studies, this may be why the A-site deficit is approximately 3 to 4 times the number of Cs atoms. However, because of uncertainties regarding the ordering of cations and vacancies at the A site and because natural pyrochlores, and presumably cesstibtantite, can have the defect pyrochlore structure as a significant component, the broader formulation is suggested.

Actual formulae for the cesstibtantite samples used in the structure analyses are:
(1) Leshaia (KO-1):

$$A_{0.91}B_2O'_6(\phi, A')_{1.00}$$

where $A = 0.57\ Sb^{3+} + 0.31\ Na + 0.02\ Pb + 0.01\ Bi^{3+}$
$B = 1.88\ Ta + 0.12\ Nb$
$O' = 5.69\ O + 0.31\ (OH + F)$
$\phi = 0.69\ (OH + F)$
$A' = 0.31\ Cs$

(2) Tanco (SMP-6):

$$A_{1.06}B_2O'_6(\phi, A')_{0.78}$$

where $A = 0.45\ Na + 0.39\ Sb^{3+} + 0.14\ Pb + 0.06\ Ca + 0.02\ Bi^{3+}$
$B = 1.95\ Ta + 0.05\ Nb$
$O' = 5.78\ O + 0.22\ (OH + F)$
$\phi = 0.55\ (OH + F)$
$A' = 0.22\ Cs + 0.01\ K$

3. Lone-pair cations such as Sb^{3+} are positionally disordered about the ideal A site, fractionally occupying a 96*g* position. For cesstibtantite, considerable solid solution exists between Sb^{3+}, Na and Pb^{2+}, the latter of which does not show lone-pair character. It is interesting that the species cesplumtantite (*Voloshin* et al., 1986) has a different space group and apparently different stoichiometry than cesstibtantite, and therefore has a different structure. To what extent bonding tendencies of Sb^{3+} versus Pb^{2+} regulate these differences is not known; the cesplumtantite structure is still unknown.
4. The mean separation of the A and A' sites is too short to represent a stable Sb-Cs separation. This indicates that the refined structure is an average. Two possibilities exist for the real structure, and depend upon the range of ordering of A and A' cations versus vacancies. (1) *Short-range order.* The low fractional cation occupancies of the A' and ϕ sites permit a model in which the mineral consists of domains with A' cations but no A cations, and *vice-versa.* In this case the mineral would consist of domains of both normal and inverse pyrochlore structure. (2) *Long-range order.* The structure would consist of a pyrochlore-like BO_6 octahedral framework with undefined cation-vacancy ordering at what are presently termed the A and A' sites.
5. Cesstibtantite possesses a small subset of X-ray reflections which normal pyrochlores do not typically have. Conversely stated, these reflections will be systematically absent for normal pyrochlores with all atoms at ideal positions. Displacement of the A cations off the $\bar{3}$ axis to a 96*g* site relaxes these conditions, and constructive scattering is observed from the planes given in Table 5. These reflections should be indigeneous to all pyrochlores with A cations having stereoactive lone pairs of electrons, and conversely should be useful indicators of the presence of such cations in pyrochlores. Because the A-cation displacements are not due to $A' - A$ cation repulsion, they cannot be used as an indirect indication of inverse-pyrochlore character, contrary to earlier suggestions (*Ercit* et al., 1985).

Acknowledgements

The authors thank *E. H. Nickel, M. Novak* and *A. V. Voloshin* for sample loans, the Tantalum Mining Corporation of Canada for permitting access to the underground workings of the

Tanco pegmatite, and Tanco mine geologists *R. A. Crouse* and *P. Vanstone* for their guidance with underground activities. Financial support for the study was in the form of a NSERC operating grant, DEMR Research Agreement, and a Tantalum Mining Corporation of Canada contract to PČ, a NSERC equipment grant to FCH and a NSERC Postgraduate Scholarship, University of Manitoba fellowships and Canadian Museum of Nature operational funds to TSE.

References

Appleman DE, Evans HT (1973) Job 9214: Indexing and least-squares refinement of powder diffraction data. US National Technical Information Service, PB 216 188

Bernotat-Wulf H, Hoffmann W (1982) The crystal structures of lead niobates of the pyrochlore type. Z Kristallogr 158: 101–117 (in German)

Birchall T, Sleight AW (1975) Nonstoichiometric phases in the Sn-Nb-O and Sn-Ta-O systems having pyrochlore-related structures. J Solid State Chem 13: 118–130

Colby JW (1980) MAGIC V—a computer program for quantitative electron-excited energy dispersive analysis. In: QUANTEX-Ray Instruction Manual. Kevex Corporation, Foster City

Eid AS, von Knorring O (1976) Geochemical aspects of the tantalum mineral microlite from some African pegmatites. Res Inst Afr Geol, Univ Leeds, Ann Rpt 20: 56–58

Ercit TS (1986) The Simpsonite Paragenesis. The Crystal Chemistry and Geochemistry of Extreme Ta Fractionation. Thesis, University of Manitoba, Winnipeg

— *Černý P, Hawthorne FC* (1985) Normal and inverse pyrochlore group minerals. Geol Assoc Canada. Prog with Abstr 10: A17

— *Hawthorne FC, Černý P* (1986) The crystal structure of bobfergusonite. Can Mineral 24: 605–614

English AD, Sleight AW (1980) ^{205}Tl and ^{19}F NMR study of ionic motion and structure in a series of thallium pyrochlore ionic conductors. Mat Res Bull 15: 1727–1735

Fourquet JL, Jacoboni C, de Pape R (1973) Les pyrochlores $A^1B_2O_6$: Mise en évidence de l'occupation par le cation A^1 de nouvelles positions cristallographiques dans le groupe d'espace Fd3m. Mat Res Bull 8: 393–404

Grins J, Nygren M, Wallin T (1980) Studies on composition, structure and ionic conductivity of the pyrochlore type system $K_{1+x}Ta_{1+x}W_{1-x}O_6 \cdot nH_2O$, $0 \leq x \leq 1$. Mat Res Bull 15: 53–61

Groult D, Pannetier J, Raveau B (1982) Neutron diffraction study of the defect pyrochlores $TaWO_{5.5}$, $HTaWO_6$, $H_2Ta_2O_6$, and $HTaWO_6 \cdot H_2O$. J Solid State Chem 41: 277–285

Hogarth DD (1977) Classification and nomenclature of the pyrochlore group. Am Mineral 62: 403–410

Jeanne G, Desjardin G, Raveau B (1974) Synthèse et évolution structurale de nouveaux pyrochlores au bismuth. Mat Res Bull 9: 1321–1332

Nickel EH, Robinson BW (1985) Kimrobinsonite, a new tantalum mineral from Western Australia, and its association with cesstibtantite. Can Mineral 23: 573–576

Oyetola S, Verbaere A, Piffard Y, Tournoux M (1988) The layered compounds $AM^V(PO_4)_2$ (A = K, Rb, Cs and M = Sb, Nb, Ta). Eur J Solid State Inorg Chem 25: 259–277

Piffard Y, Dion M, Tournoux M (1978) Structure cristalline du pyrochlore, $K_{.51}Sb_{.67}Sb_2O_{6.26}$. Acta Cryst B34: 366–368

Rucklidlge J, Gasparrini E (1969) Electron Microprobe Analytical Data Reduction (EMPADR VII). Dept of Geology, Univ of Toronto, Toronto

Schrewelius N (1943) A Study of Antimonates, Hydroxyantimonates and Fluorantimonates. Thesis, Univ of Stockholm, Stockholm (in Swedish)

Shannon, RD (1976) Revised effective ionic radii and systematic studies of interatomic distances in halides and chalcogenides. Acta Cryst A32: 751–767

Stewart DJ, Knop O, Ayasse C, Woodhams FWD (1972) Pyrochlores. VII. The oxides of antimony: an X-ray and Mössbauer study. Can J Chem 50: 690–700

Subramanian M A, Aravamudan G, *Subba Rao GV* (1983) Oxide pyrochlores—a review. Prog Solid State Chem 15: 55—143

Voloshin AV, Men"shikov YuP, Pakhomovskii YaA, Polezhaeva LI (1981) Cesstibtantite, (Cs, Na)$SbTa_4O_{12}$—a new mineral from granitic pegmatites. Zap Vses Mineral Obshch 116: 345–351 (in Russian)

— *Pakhomovskii YaA, Bakhchisaraitsev AYu, Devinia II* (1986) Cesplumtantite——a new cesium-antimony tantalate from granitic pegmatites. Mineral Zhur 8(5): 92–98 (in Russian)

Authors' addresses: *T. S. Ercit*, Canadian Museum of Nature, P.O. Box 3443, Station "D", Ottawa, Ontario, Canada K1P 6P4; *P. Černý* and *F. C. Hawthorne*, Department of Geological Sciences, Wallace Building, University of Manitoba, Winnipeg, Manitoba, Canada R3T 2N2